Journal of Materials Processing Technology 233 (2016) 100–106

Contents lists available at ScienceDirect

Journal of Materials Processing Technology

journal homepage: www.elsevier.com/locate/jmatprotec

Closed-loop control of variable layer width for thin-walled parts in wire and arc additive manufacturing

Jun Xiong[a], Ziqiu Yin[a], Weihua Zhang[b,*]

[a] School of Materials Science and Engineering, Southwest Jiaotong University, Chengdu 610031, China
[b] State Key Laboratory of Traction Power, Southwest Jiaotong University, Chengdu 610031, China

ARTICLE INFO

Article history:
Received 30 November 2015
Received in revised form 22 February 2016
Accepted 24 February 2016
Available online 2 March 2016

Keywords:
Additive manufacturing
Wire and arc
Variable layer width
Thin-walled parts
Closed-loop controller

ABSTRACT

An intelligent single-neuron self-adjusting controller is proposed for variable layer width control in wire and arc additive manufacturing (WAAM). The travel speed is selected as the input control variable and the layer width is chosen as the output. The performance of the controller is validated by the disturbance of deposition current, inter-layer temperature, and given layer width. It is also evaluated through deposition of a 13-layered wall with variable layer width. The proposed controller is effective for increasing the process stability when the expected layer width ranges from 6 to 9 mm.

1. Introduction

With an increasing emphasis on sustainability, additive manufacturing for building metal parts offers a substantial merit in terms of decreased buy-to-fly ratios (Williams et al., 2015). In comparison to conventional subtractive manufacturing process, additive manufacturing is an additional technique for fabricating complex metal parts by adding of materials, in the form of powder or wire. A proposed approach in this field is wire and arc additive manufacturing (WAAM). Using welding arc as the heat source can offer a significant advantage of low cost for equipment. On the other hand, utilizing wire as the deposition material greatly improves material efficiencies, as all the wire is fed into the molten pool during the process.

In recent years, many researches have been focused on WAAM in terms of forming technology and metallurgical properties. For instance, Martina et al. (2012) investigated the forming geometry and microstructure of thin-walled Ti-6Al-4V parts deposited by plasma arc plus wire. In Baufeld et al. (2010), microstructure and mechanical properties of Ti-6Al-4V components fabricated by gas tungsten arc welding were investigated. Microstructure and residual stress of parts, built by metal inert gas welding, were improved by means of high-pressure rolling (Colegrove et al., 2013). As described in Martina et al. (2015), depositing Ti-6Al-4V parts with high-pressure interpass rolling can reduce the overall thickness of α phase lamellae and change the microstructure from strongly columnar to equiaxed. Effects of process variables on forming appearance were studied in WAAM through a passive vision sensor (Xiong et al., 2015), indicating that the deposition current was the major factor.

It is known that WAAM is a multi-variable and strongly coupled process, which is susceptible to small variations in process parameters, such as the arc current, arc voltage, and travel speed. As a consequence, changes in parts geometry and quality are inevitably produced in WAAM, even with identical process variables. Moreover, disturbances, including the inter-layer temperature, heat elimination condition, and previous forming geometry, have significant effects on the current layer geometry. Some control strategies, such as control of inter-layer temperature by natural cooling (Spencer et al., 1998), control of arc striking and extinguishing appearance through adjusting process parameters (Zhang et al., 2003), and combining additive manufacturing and milling process to improve the surface smoothness of components (Karunakaran et al., 2010), have been proposed to improve the forming quality. However, layer geometry variations, resulted from fluctuations in process parameters and work environment, cannot be eliminated by an open-loop control system. It is necessary to establish a closed-loop control system for WAAM.

* Corresponding author at: State Key Laboratory of Traction Power, Southwest Jiaotong University, 111, Section 1 North Second Ring Road, Chengdu 610031, China.
E-mail addresses: xiongjun@home.swjtu.edu.cn (J. Xiong), changfeng000007@163.com (W. Zhang).

http://dx.doi.org/10.1016/j.jmatprotec.2016.02.021
0924-0136/

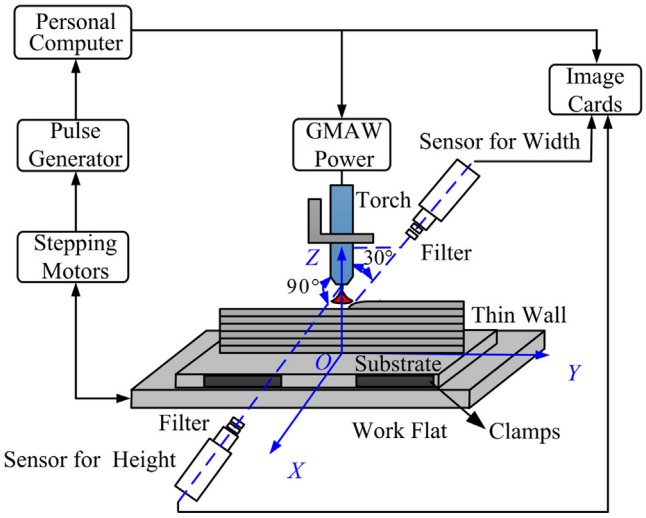

Fig. 1. The schematic diagram of WAAM system.

From the available literatures, effective detection and control methods for layer geometry in WAAM have not been developed in depth. Doumanidis and Kwak (2002) established a multi-variable adaptive control system in WAAM through an active vision sensor that can produce a large detection lad. As described in Heralic et al. (2012), height control in laser metal-wire deposition was realized based on iterative learning control. By contrast, several publications have been reported in powder-based deposition process, e.g. height control through a feedforward proportional-integral-derivative (PID) controller (Fathi et al., 2007), layer-to-layer height control for laser metal deposition process using iterative learning control (Tang and Landers, 2011).

In our previous study, a passive vision system for layer width and height detection has been designed (Xiong and Zhang, 2013). This paper aims at realizing an interesting variable width control for various layers in WAAM through a closed-loop control system. The thin-walled structure is chosen to evaluate the effectiveness of the proposed controller.

2. Experimental details

WAAM system is mainly composed of a gas metal arc welding power supply, a moveable workflat, a visual-sensing system, and a personal computer for control, as presented in Fig. 1. The power supply was Panasonic YD-500FR. The deposition torch was fixed on a slide rail. Gas metal arc, struck between the wire electrode and the top surface of the thin wall, was used as the heat source. The shielding gas was 95% Ar and 5% CO_2 with a flow rate of 18 L/min, with a view to protecting the molten pool. The wire electrode with the diameter of 1.2 mm was H08Mn2Si, which is a trademark of wire made in China. The geometry of the mild steel substrate was 260 mm × 80 mm × 9.5 mm. Table 1 presents the composition of the electrode wire and substrate. It should be noted that if no special instructions, the deposition current was set at 150 A, and the arc voltage was 22 V.

The work flat, driven by two stepping motors, can move in the Y-axis and lift in the Z-axis, respectively. During the process, the torch was kept fixed, and thin-walled parts were built by the movement of the workflat along the Y-axis. As one layer was performed, the arc was extinguished and the work flat was made a descent by a given layer height along the Z-axis. Then, another layer was begun to be deposited.

The personal computer with a data acquisition and an image grabbing card was the center of the control system. It was responsible for arc on/off, adjusting wire feed rate as well as travel speed, and displaying sensing images.

As seen in Fig. 1, a passive vision sensor, consisting of a neural filter, a narrow-band filter with center wavelength of 650 nm, and a CCD camera, was used for layer width detection. The vision sensor for width detection was mounted on the rear of the torch. Due to multi-layer depositions, the distance between the nozzle and the top surface of the thin wall is variable. Consequently, the calibration of the sensor system is difficult. In this circumstance, another vision sensor system with the same optical components was applied to monitor the nozzle to the top surface distance. The detailed image processing algorithms and calibration procedures can refer to Xiong and Zhang (2013). The flow chart of image processing is presented in Fig. 2.

Table 2
Time constant, time-delay, and gain coefficient of layer width with travel speed step.

Positive step	K	−0.689
	T_s	0.5933
	T_d	1.0
Negative step	K	−1.1035
	T_s	1.783
	T_d	1.4

3. System identification

Generally, a control system is composed of dynamic characteristics of the controlled object and the controller design. The principle of the controller design is to devise reasonable control algorithms for acquiring the excellent performance index of the controller, through establishing a dynamic model of the process. As a consequence, it is essential to develop the dynamic model relating the controlling and controlled variables. In this research, the travel speed is selected as the control input, and the output is the layer width.

At first, step response experiments were conducted to study the dynamic characteristics of WAAM process. It was achieved by performing a step change in the travel speed. After depositing three layers on the substrate, the step response experiment was conducted on the fourth layer. As seen in Fig. 3, the positive step of the travel speed increases from 5 to 7 mm/s, and the negative step decreases from 7 to 5 mm/s. It is demonstrated that the travel speed has a negative effect on the layer width. The response of layer width under the step change has no overshoot. Therefore, WAAM can be assumed as a first-order process, the transfer function of which can be formulated as:

$$G(s) = \frac{K}{1+T_s} e^{-\tau s} \quad (1)$$

where K is the static gain, τ is the time-delay constant, and T_s is the time constant.

The coefficients of the transfer function models are displayed in Table 2. The deposition process for layer width has a certain time-

Table 1
Composition of experiment materials (wt.%)

Materials	C	Mn	Si	Cr	Ni	S	P	Fe
Wire	0.06–0.15	1.8–2.1	0.65–0.95	≤0.2	≤0.3	≤0.025	≤0.025	Reminder
Substrate	0.12–0.2	0.3–0.7	≤0.3	≤0.3	≤0.3	≤0.045	≤0.045	Reminder

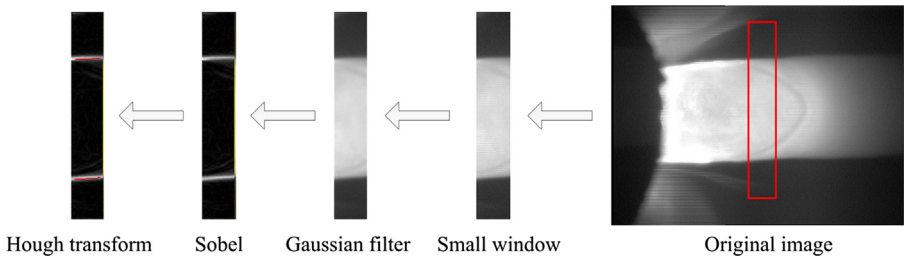

Fig. 2. Development of image processing procedure for deposited layer width.

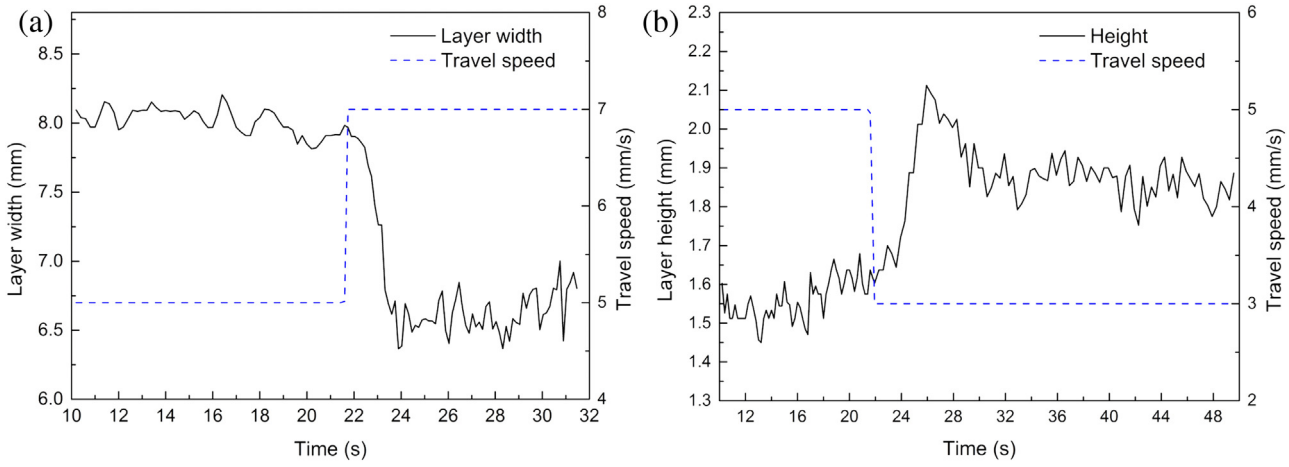

Fig. 3. Transient response of layer width to travel speed. (a) Positive step. (b) Negative step.

delay and nonlinearity. The time constant, time-delay, and gain coefficient in positive and negative steps are various. The process cannot be simply formulated with a transfer function. It is necessary to establish a more accurate model to present the dynamic characteristics of the layer width in WAAM process.

A non-linear Hammerstein model was utilized to establish the dynamic relationship between the layer width and travel speed. This model is composed of a linear dynamic and a nonlinear memoryless submodel. The system model can be expressed as:

$$y(k) = x(k)z^{-d}B(z^{-1})/A(z^{-1}) \tag{2}$$

where $x(k) = C_0 + C_1u(k) + C_2u^2(k)$, $z^{-d}B(z^{-1})/A(z^{-1})$ is the linear dynamic link, $y(k)$ is the layer width, $u(k)$ is the travel speed, z^{-1} is the delay operator. $A(Z^{-1})$ and $B(Z^{-1})$ are polynomials written as:

$$A(z^{-1}) = 1 + a_1z^{-1} + a_2z^{-2} + \cdots + a_{n_a}z^{-n_a} \tag{3}$$

$$B(z^{-1}) = b_0 + b_1z^{-1} + b_2z^{-2} + \cdots + b_{n_b}z^{-n_b} \tag{4}$$

where n_a and n_b are structural parameters.

With a view to obtaining input-output data, the travel speed has to be changed randomly in a certain range for continuously stimulating the deposition process. The travel speed was varied randomly between 3 to 8 mm/s, as shown in Fig. 4(a). The sampling period was set at 0.5 s, which was calculated by the time and time-delay constant. Four groups of experiments were performed, and about 280 useful sampling points are obtained by removing points located in the arc striking and extinguishing area. The corresponding layer width is given in Fig. 4(b).

On the basis of the input-output data shown in Fig. 4, the structure parameters of the Hammerstein model were calculated by means of the block least square approach (Ljung, 1999), namely, $n_a = 4$, $n_b = 4$, $d = 2$. Therefore, the dynamic characteristics between the travel speed and layer width can be written as:

$$\begin{aligned} y(k) &= 0.419y(k-1) - 0.075y(k-2) - 0.039y(k-3) \\ &\quad -0.03y(k-4) + 0.069 \\ &-0.079u(k-2) - 0.17u(k-3) - 0.087u(k-4) - 0.095u(k-5) \\ &-0.03u(k-6) - 0.038u^2(k-2) - 0.02u^2(k-3) + 0.01u^2(k-4) \\ &+0.004u^2(k-5) + 0.019u^2(k-6) \end{aligned} \tag{5}$$

4. Controller design

Considering that WAAM is a nonlinear process with multivariable. Interference factors, including the sensitivity in arc current and voltage, heat dissipation condition, and inter-layer temperature, are various. A conventional PID feedback controller with fixed parameters cannot always keep an optimum control effect. Thus, a controller with parameters self-regulation is necessary. In this research, a single-neuron controller (Marsik, 1983) was developed for the layer width control. It can form a self-learning control system by monitoring the actual and expected output. To keep the output of the control system excellent, the weights of the neuron are adjusted by the back propagation algorithm.The inputs of the single neuron can be expressed as:

$$\begin{aligned} h_1(t) &= \Delta e(t) = e(t) - e(t-1) \\ h_2(t) &= e(t) \\ h_3(t) &= \Delta^2 e(t) = \Delta h_1(t) = h_1(t) - h_1(t-1) \end{aligned} \tag{6}$$

where $e(t) = W_{set}(t) - W_b(t)$, which is the error of the output.

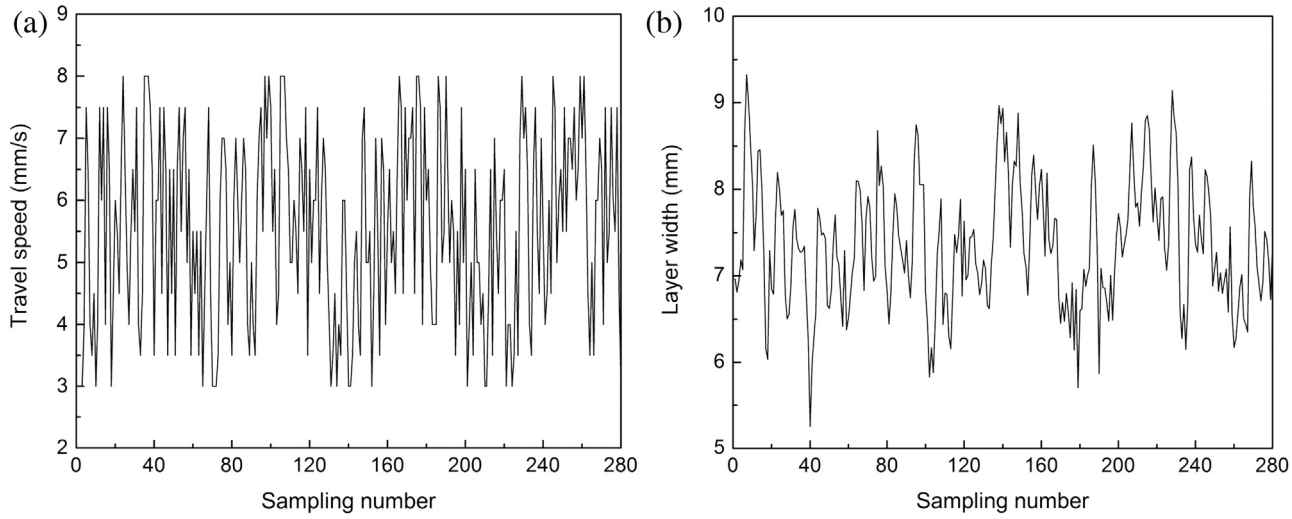

Fig. 4. Experimental transient response of the deposition process using a random travel speed. (a) Travel speed. (b) Layer width.

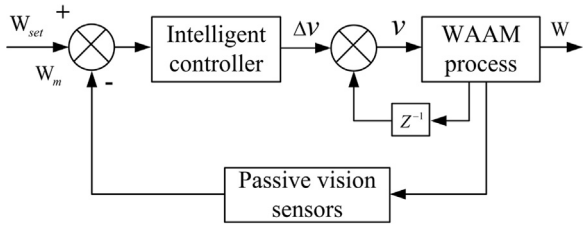

Fig. 5. Schematic diagram of single-neuron self-learning controller for layer width in WAAM.

The weight sum of three nodes is calculated as:

$$o(t) = \sum_{i=1}^{3} w_i(t)h_i(t) / \sqrt{\sum_{i=1}^{3} w_i^2(t)} \quad (7)$$

To obtain a smooth output, S-function is introduced. The output of the controller is given by:

$$\Delta\delta(t) = \delta_{\max} \frac{1 - e^{-o(t)}}{1 + e^{-o(t)}} \quad (8)$$

The performance index can be written as:

$$J(t) = 0.5[W_{bset} - W_b(t)]^2 \quad (9)$$

Learning algorithms of the weights are calculated as:

$$\Delta w_i(t) = -\frac{\partial J}{\partial w_i(t)} = e(t)\frac{\partial W_b(t)}{\partial \Delta\delta(t)}\delta_{\max}[1 - \Delta\delta^2(t)/\delta_{\max}^2]h_i(t) \quad (10)$$

where $\frac{\partial W_b(t)}{\partial \Delta\delta(t)} \approx \frac{W_b(t) - W_b(t-1)}{\Delta\delta(t) - \Delta\delta(t-1)}$.

The schematic diagram of single-neuron self-learning controller for layer width in WAAM is shown in Fig. 5, in which the input of the controller is an offset between the detected and given layer width, and the output is the travel speed. The detecting component for the layer width is the passive vision sensor, and all of them form the closed-loop control system for the layer width control in WAAM.

5. Experimental results and discussion

5.1. Performance verification for controller

Before applying the developed controller to actual process, the performance of the controller should be verified by simulation or real disturbance tests. Firstly, the control process was simulated by the controller design and the developed dynamic model. The simulation program was carried out by MATLAB language, and the result is given in Fig. 6. The initial layer width is 7.6 mm, and the travel speed is 5.5 mm/s. The expected layer width is given a step change to 8.5 mm/s. Considering that the control system has a certain delay, the overshoot has to be reduced for increasing the stability of the

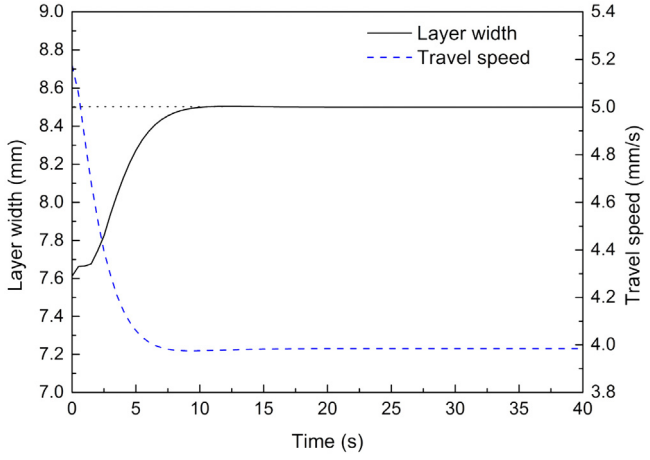

Fig. 6. Simulation curves of the single-neuron self-learning controller.

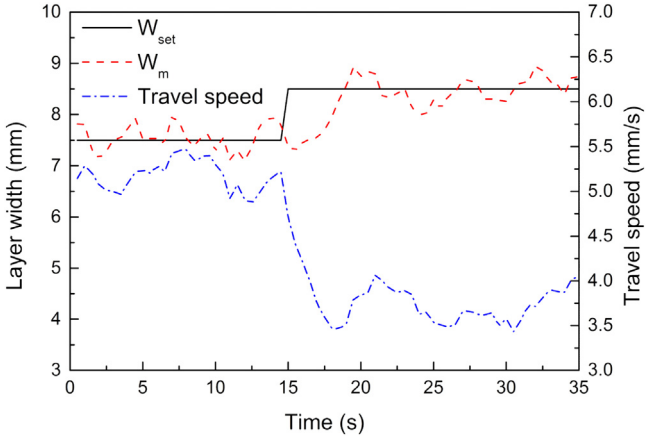

Fig. 7. Closed-loop control with a disturbance of given width.

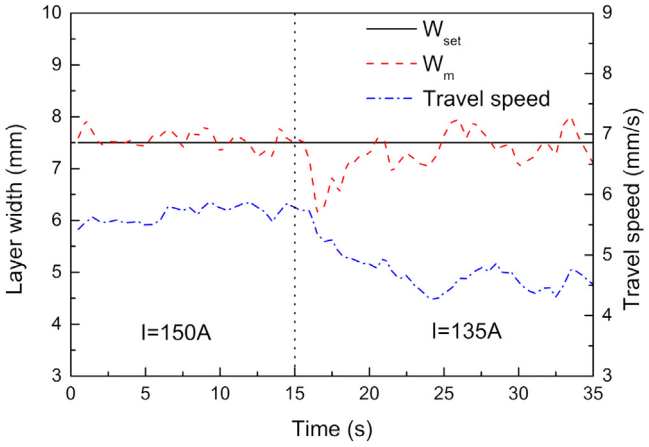

Fig. 8. Closed-loop control with a disturbance of deposition current.

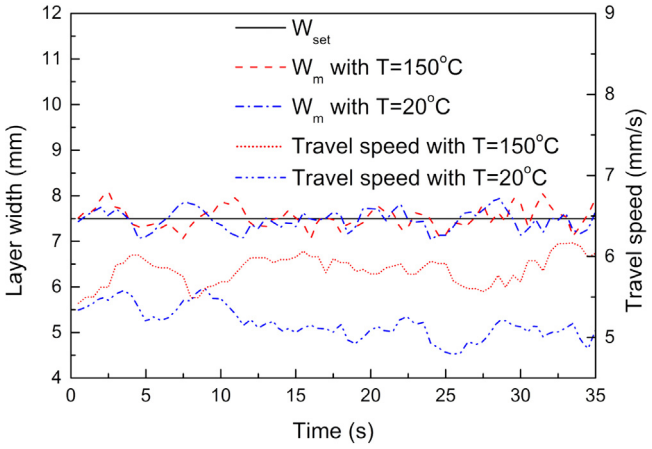

Fig. 9. Closed-loop control with a disturbance of inter-layer temperature.

control system. It can be seen in Fig. 6 that the maximum overshoot is 0.04%, and the settling time is less than 8 s.

To validate the actual performance of the controller, several interference tests were devised. Fig. 7 shows the control effect of the single-neuron self-learning controller with the disturbance of the given layer width. The sampling and control period were both 0.5 s. At $t = 15s$, the given layer width is applied a step change from 7.5 to 8.5 mm. It needs approximately 5 s for the control system to arrive the new given layer width. The measured layer width fluctuates around 8.5 mm, and the maximum error between the detected and given value is less than 0.5 mm.

Fig. 8 shows the control effect of the single-neuron self-learning controller with the disturbance of deposition current. At $t = 15s$, the deposition current decreases from 150 to 135 A. Due to the thermal inertia of the molten pool, the layer width begins to decrease at $t = 16s$. Moreover, the control effect is performed at $t = 17s$ thanks

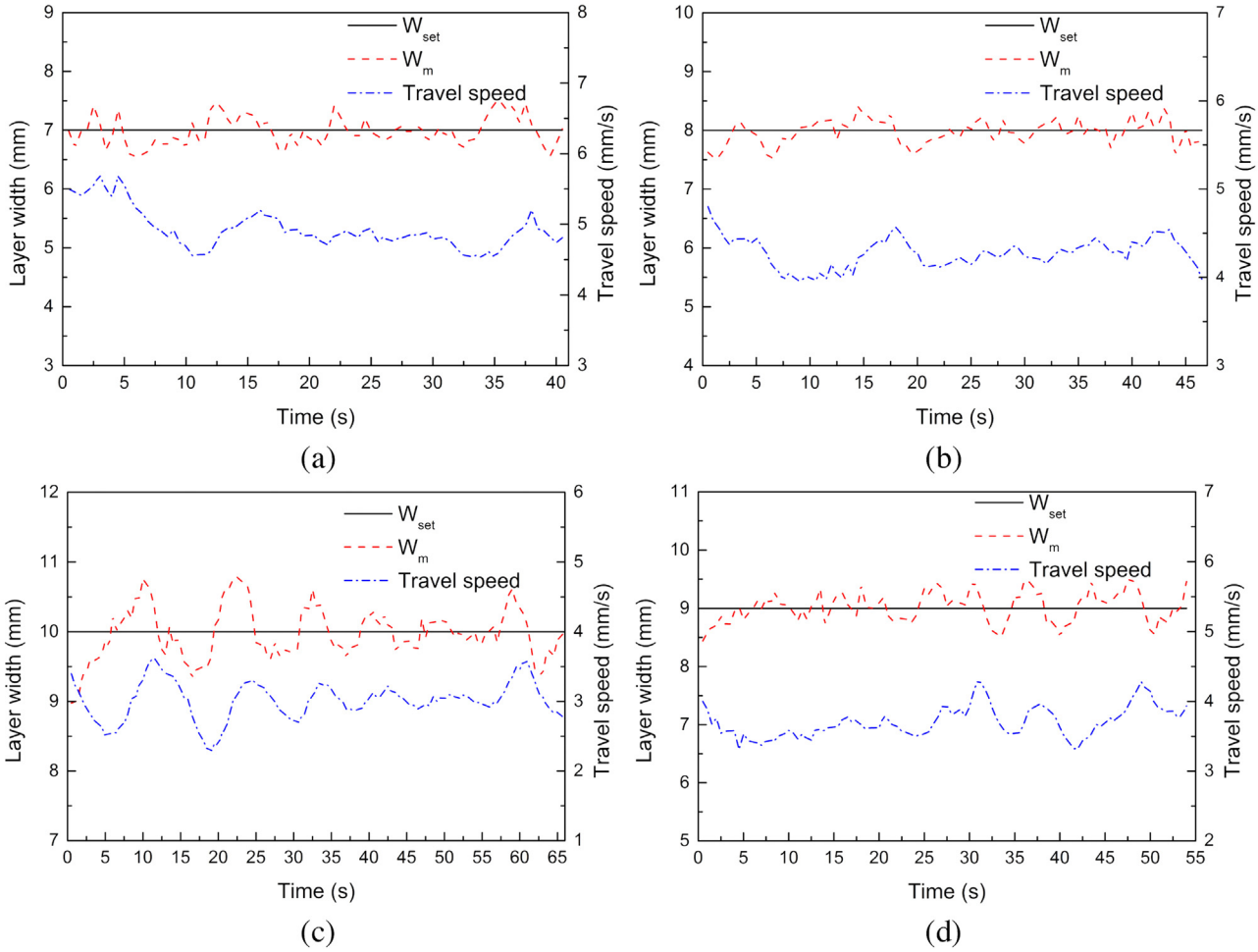

Fig. 10. Closed-loop control of variable width with a step of 1.0 mm in multi-layer single-bead WAAM process. (a) Third layer. (b) Fourth layer. (c) Sixth layer. (d) Thirteenth layer.

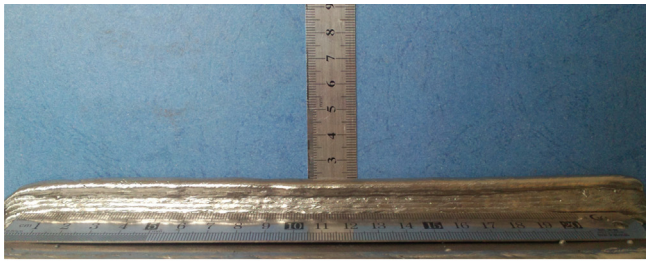

(a)

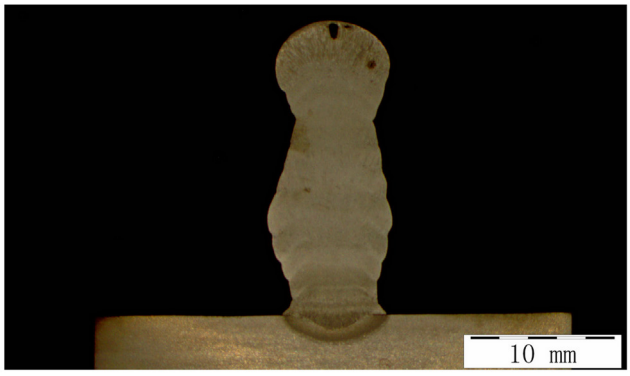

(b)

Fig. 11. Photograph and macrophotograph of the thin-walled part. (a) Forming appearance. (b) Macrophotograph.

to the lag of the control system. It is shown that the travel speed decreases with the negative step of the deposition current. The curve of the measured layer width fluctuates around the given layer width, and no large overshoot is observed.

Fig. 9 shows the control effect of the single-neuron self-learning controller with the disturbance of inter-layer temperature. A 10-layered wall was deposited. The inter-layer temperatures of 6th and 9th layers were controlled at 150 and 20 °C, respectively. Closed-loop controller tests were performed on the 7th and 10th layer, respectively. As presented in Fig. 9, the given layer width is 7.5 mm, and detected curves of layer width with different inter-layer temperatures are varied around the given width. The travel speed with inter-layer temperature of 150 °C is larger than that with inter-layer temperature of 20 °C. This is because other process parameters being equal, the width of the molten pool increases along with the inter-layer temperature. As a consequence, the travel speed with inter-layer temperature of 150 °C has to increase to maintain the given layer width.

5.2. Variable layer width control

In this section, the single-neuron self-learning controller is utilized for variable width control for a thin-walled part. Namely, the layer widths in different layers are various. A 13-layered wall with a step change of 1 mm in layer width was deposited. The width of the second layer was set at 6 mm. With the increase in the number of layers, the layer width firstly increased to 10 mm, then decreased to 6 mm, and then increased to 9 mm. The deposition length of the wall was about 250 mm. To decrease the regulating time and increase the stability of the controller, the initial travel speed in each layer was set based on experiences.

Using the closed-loop controller, the detected width and corresponding travel speed in different layers are presented in Fig. 10. It can be shown that deviations in layer width are approximately limited to 0.5 mm except for the six layer. The mean square errors in Fig. 10 are 0.2435 mm, 0.1909 mm, 0.3405 mm, 0.2492 mm, respectively. It is shown that the fluctuations in detected width and travel speed increase along with the given layer width. Furthermore, the time between adjacent peaks increases with increasing the given layer width, particularly that shown in Fig. 10(c). The reason is that the area detected by the passive vision sensor is approximately 18 mm away from the deposition torch. Provided that the expected layer width is larger, the travel speed calculated by the closed-loop controller is smaller, leading to a larger lag of the detection system and a less stability of the control system. Thus, the optimal expected layer width ranges between 6 and 9 mm. The photograph of the deposited wall is shown in Fig. 11(a). The macrophotograph of variable width control with a step of 1.0 mm in multi-layer single-bead is presented in Fig. 11(b).

6. Conclusions

This paper aims at variable layer width control in WAAM process through deposition of thin-walled parts. Conclusions drawn from this study are listed below.

- WAAM is a nonlinear process, and the dynamic model between layer width and travel speed can be established by a second-order Hammerstein model.
- An intelligent controller was developed for an interesting variable width control in different layers. The maximum absolute error between the detected and expected width was less than 0.5 mm except that the layer width was set at 10 mm
- When using the travel speed as the controlling variable, the optimal given layer width ranges between 6 to 9 mm to reduce the overshoot of the control system.

Acknowledgments

This work was funded by National Natural Science Foundation of China, no. 61573293 and no. 51505394, China Postdoctoral Science Foundation, no. 2015M580796, and the Key Technologies R&D Program of Sichuan Province, China, no. 2015GZ0305.

References

Baufeld, B., Biest, O.V.D., Gault, R., 2010. Additive manufacturing of Ti-6Al-4V components by shaped metal deposition: microstructure and mechanical properties. Mater. Des. 31, S106–S111.

Colegrove, P.A., Coules, H.E., Fairman, J., Martina, F., Kashoob, T., Mamash, H., Cozzolino, L.D., 2013. Microstructure and residual stress improvement in wire and arc additively manufactured parts through high-pressure rolling. J. Mater. Process. Technol. 213 (10), 1782–1791.

Doumanidis, C., Kwak, Y.M., 2002. Multivariable adaptive control of the bead profilegeometry in gas metal arc welding with thermal scanning. Int. J. Press. Vessels Pip. 79, 251–262.

Fathi, A., Khajepour, A., Toyserkani, E., Durali, M., 2007. Clad height control in laser solid freeform fabrication using a feedforward PID controller. Int. J. Adv. Manuf. Technol. 35, 280–292.

Heralic, A., Christiansson, A.K., Lennartson, B., 2012. Height control of laser metal-wire deposition based on iterative learning control and 3D scanning. Opt. Lasers Eng. 50, 1230–1241.

Karunakaran, K.P., Suryakumar, S., Pushpa, V., Akula, S., 2010. Low cost integration of additive and subtractive processes for hybrid layered manufacturing. Rob. Comput. Integr. Manuf. 26, 490–499.

Ljung, L., 1999. System Identification: Theory for the User. Prentice Hall, Englewood Cliffs, NJ.

Marsik, J., 1983. A new conception of digital adaptive PSD control. Prob. Control Inf. Theory 12 (4), 267–279.

Martina, F., Mehnen, J., Williams, S.W., Colegrove, P., Wang, F., 2012. Investigation of the benefits of plasma deposition for the additive layer manufacture of Ti-6Al-4V. J. Mater. Process. Technol. 212, 1377–1386.

Martina, F., Colegrove, P.A., Williams, S.W., Meyer, J., 2015. Microstructure of interpass rolled wire plus arc additive manufacturing Ti-6Al-4V components. Metall. Mater. Trans. A 46A (12), 6103–6118.
Spencer, J.D., Dickens, P.M., Wykes, C.M., 1998. Rapid prototyping of metal parts by three-dimensional welding. Proc. Inst. Mech. Eng. B: J. Eng. Manuf. 212, 175–182.
Tang, L., Landers, R.G., 2011. Layer-to-layer height control for laser metal deposition process. J. Manuf. Sci. Eng.-Trans. ASME 133 (021009-1–021009-9).
Williams, S.W., Martina, F., Addison, A.C., Ding, J., Pardal, G., Colegrove, P., 2015. Wire+Arc additive manufacturing. Mater. Sci. Technol., http://dx.doi.org/10.1179/1743284715Y.0000000073.
Xiong, J., Zhang, G.J., 2013. Online measurement of bead geometry in GMAW-based additive manufacturing using passive vision. Meas. Sci. Technol. 24 (11), 115103.
Xiong, J., Zhang, G.J., Zhang, W.H., 2015. Forming appearance analysis in multi-layer single-pass GMAW-based additive manufacturing. Int. J. Adv. Manuf. Technol. 80, 1767–1776.
Zhang, Y.M., Chen, Y.W., Li, P.J., Male, A.T., 2003. Weld deposition-based rapid prototyping: a preliminary study. J. Mater. Process. Technol. 135, 347–357.